Proceedings of IDETC/CIE 2006
ASME 2006 International Design Engineering Technical Conferences &
Computers and Information in Engineering Conference
September 10-13, 2006, Philadelphia, Pennsylvania, USA

DETC2006-99687

MODELING UNCERTAINTY FOR PLANAR MESO-SCALE MANIPULATION AND ASSEMBLY

David J. Cappelleri*
GRASP Lab
Department of Mechanical Engineering
and Applied Mechanics
University of Pennsylvania
Philadelphia, PA 19104
Email: dcappell@grasp.upenn.edu

Jonathan Fink
GRASP Lab
Department of Electrical
and Systems Engineering
University of Pennsylvania
Philadelphia, PA 19104
Email: jonfink@grasp.upenn.edu

Vijay Kumar
GRASP Lab
Department of Mechanical Engineering
and Applied Mechanics
University of Pennsylvania
Philadelphia, PA 19104
Email: kumar@grasp.upenn.edu

ABSTRACT

While robotic assembly at the centimeter and meter length scale is well understood and is routine in the manufacturing industry, robotic grasping and manipulation for meso-scale assembly at the millimeter and sub-millimeter length scales are much more difficult. This paper explores an possible way to manipulate and assemble planar parts using a micro-manipulator with a single probe capable of pushing parts on a planar surface with visual feedback. Specifically, we describe a study of the uncertainty associated with planar surface friction with a goal of developing a model of manipulation primitives that can be used for assembly. We describe a series of experiments and data analysis algorithms that allow us to identify the main system parameters for quasi-static operation, including the friction coefficient and the force distribution, while characterizing the uncertainty associated with these parameters. This allows us to bound the range of motions resulting from the uncertainty, which is necessary to design robust open-loop meso-scale manipulation and assembly motion plans.

INTRODUCTION

While there are many examples of miniaturized products that are produced using highly automated processes, most of these processes involve hard automation or the use of specialized equipment for assembly. In contrast to macro-scale assembly which is now performed using general purpose robots for many products, it is much more difficult to design general purpose manipulation or assembly processes for micro-scale parts. There are several reasons for this. Inexpensive and reliable sensors are non-existent at this scale. It is difficult to measure forces at the micro-netwon level using off-the-shelf force sensors and good force-feedback control schemes have not proved successful. It is hard to manufacture general-purpose end effectors at this scale and it is even more difficult to grasp and manipulate parts at the micro and meso level than it is at the macro level. Finally, the lack of good models of the mechanics of contact interactions at this scale means that model-based approaches to control of micro and meso manipulation are difficult.

The problem of designing open-loop plans for simple end effectors using manipulation primitives that do not require precise real-time feedback to accomplish planar manipulation tasks has been investigated before [1–3]. In [4], we investigated a meso-scale assembly task, as shown in Figure 1. It involves planar movement and reorientation of a 1600×850 μm part (peg) from an initial configuration (A) to a final configuration (B) through a 1000 μm wide channel. We designed and experimentally verified open-loop plans for a simple four degree-of-freedom micro-manipulator with a probe to manipulate planar parts on an inverted microscope. We found that these manipulation plans were not robust to errors resulting from the uncertainty in the model.

*Address all correspondence to this author.

This uncertainty came from three sources: (a) the force distribution or the pressure distribution across the contact between parts and the surface they rest on; (b) the coefficient of friction between the part and the contacting surface; and (c) the coefficient of friction between the probe and the manipulated part. While it is possible to measure these parameters in a laboratory setting, it is difficult to directly measure these parameters just before or while performing the task.

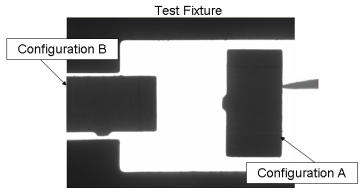

Figure 1. Typical meso-scale assembly task: Move part from configuration A to configuration B.

This paper explores a methodology for experimentally characterizing this uncertainty associated with these three sets of parameters without directly measuring these parameters and without any special sensors. We describe a series of experiments and data analysis algorithms designed to experimentally identify these system parameters, with the goal of using these parameters and an estimate of the underlying uncertainty for manipulation and assembly.

RELATED WORK

Gripping and manipulation techniques for micro-assembly applications is an active area of research [5]. Specifically, there is a body of work pertaining to pick-and-plance micro-assembly tasks using micro-gripping techniques and strategies [6–11]. Our focus is rather on micro-scale pushing operations, which are better suited for open-loop manipulations.

The derivation of the fundamental mechanics of pushing operations and sliding objects have been extensively studied by [12–14]. There is also extensive work addressing the analysis and simulation of mechanical systems with frictional contacts. In particular, semi-implicit and instantaneous-time models for predicting motion and contact forces for quasi-static multi-rigid-body systems have recently been developed [15, 16].

Pushing operations and the instantaneous motions of a sliding object during multiple contact pushing is examined and the manipulation primitive of stable rotational pushing is defined in [17]. In [18], the bounds of the possible motions of a pushed object are investigated. [19] presents a comparison between the dynamic and quasi-static motions of a push object.

The problem of planning pushing paths using stable pushes is discussed in [20]. A pushing control system with visual feedback for open-loop pushing is described in [21] as a way to mitigate the instability of pushing with point contacts. Open-loop motion strategies, without the use of sensors, can be used to eliminate uncertainty and to orient polygonal parts [1, 2, 22]. In [1], planar parts are considered polygons if their convex hull is a polygon. Given a list of n vertices describing the polygonal part with an unknown initial orientation, the shortest sequence of mechanical parallel-jaw gripper actions that will guarantee the orientation of the part up to symmetry is determined. In [2], a randomly oriented planar object is dropped into a tray. Then, using the mechanics of sliding, an automatic planner is created. The planner finds a sequence of tilting operations to leave the object's orientation completely determined. In [22], the authors study the problem of posing a planar part given initial and goal poses. Specifically, they prove that a multiple push strategy always exists (in the absence of obstacles) and they develop a complete, polynomial-time algorithm to design one possible plan. Other motion planning techniques have been applied to planning pushing paths with the presence of obstacles [23] as well as for multiple manipulators and obstacles [24]. To remove the uncertainty associated with robot pushing tasks, [25] establishes stable orientation and positions by pushing objects with two-point fingers.

For micro-scale manipulation, sticking effects due to Van der Walls forces and static electricity make the manipulator motions and part release more complicated [26, 27]. Micro-manipulators also have limited degrees of freedom when compared to manipulators at the macro-scale. These problems are addressed in [3] with a parallel-jaw gripper and squeeze and roll primitives to orient a randomly oriented polygonal part up to 180° symmetry without the use of sensors. However, in the case of the meso-scale sized parts used here, these sticking effects are not an issue since the characteristic dimensions are larger than 10 μm [28].

Estimations of friction parameters for pushed objects to improve the control of pushing has been investigated previously on larger objects and with different strategies than the ones presented here. In [29], the support surface is approximated by a discrete set of support points and experimental data is used to validate this model. It leaves the open question of how the hypothesized support points for an unknown object should be chosen. Similarly in [30], a method for estimating the friction distribution of an object and the center of friction from pushing the object several times is presented. In both of these papers, a grid system of N possible support points is applied to the base of the object being pushed. The respective algorithms determine the distribution of the normal force of the object at these support locations.

Our goal in this paper is to characterize the uncertainty associated with planar surface friction by performing friction parame-

ter estimation. A series of experiments, data analysis algorithms, and a quasi-static model of pushing are used to identify system parameters, such as choice of friction coefficient and three-point support location for a given set of manipulation tests. The uncertainty associated with these parameters and the underlying model are also explored by using these same techniques.

MANIPULATION TASK PLANNING

In this paper we address meso-scale manipulation assembly using nonprehensile manipulation primitives. As mentioned earlier, because of the lack of good grippers at the meso-scale, we are interested in using a four degree-of-freedom micro manipulator (two degrees of freedom in the plane) with a probe at the end to manipulate parts using a single frictional point contact at a time. In other words, the manipulator can only interact with the parts through pushing operations. Because of the complexity due to surface friction and intermittent frictional contacts between the part, probe, and other fixtures involved in the assembly, there is no analytical solution to the behavior of the system. However, it is possible to simulate the system and analyze the planning and control problem via simulation as in our previous work [4].

We also limit ourselves to open-loop manipulation using the paradigm that is used in industrial automation. While vision and other forms of sensing can be used for localization, placement and planning, we only consider schemes that do not require real-time feedback of position and/or forces.

Both these restrictions make the task complicated. We want plans that are robust to uncertainty in initial positioning and the dynamics. We also want to have sensors that limit the initial positioning errors and models that lend themselves to the analysis of uncertainty of both task error (initial placement of parts) and model error (estimation of parameters). It is important not only to have accurate system parameter information but also important to have error models for the system that can be used to plan the manipulation task.

Manipulation Model

Due to the scale of the system and speed of manipulation, we assume quasi-static dynamics. We use a semi-implicit time-stepping scheme [16] that is specialized to a *2.5D* problem where all parts and contact interactions are essentially planar and surface friction in the plane is modeled with a simple force distribution. All contacts are assumed to behave according to Coulomb's friction model. The interaction between the part and the supporting surface is modeled by three frictional point contacts as in [12].

Using the above assumptions, the planar manipulation system can be formulated as a mixed linear complementarity problem (MLCP) based on the following quasi-static equation of motion and time-stepping scheme for rigid bodies [4].

$$0 = W_n \lambda_n^{l+1} + W_f \lambda_f^{l+1} + F_{ext} \tag{1}$$

$$q^{l+1} - q^l = hG(q)\nu^{l+1} \tag{2}$$

where $q^l \in \mathcal{R}^{n_q}$ is the generalized configuration vector, $\nu^{l+1} \in \mathcal{R}^{n_\nu}$ is the generalized velocity vector, $G(q) \in \mathcal{R}^{n_q \times n_\nu}$ is the Jacobian matrix , $W_n \in \mathcal{R}^{n_\nu \times (n_c+n_s)}$ contains the normal wrenches for each of the $n_c + n_s$ pushing (n_c) and support (n_s) contacts. $W_f \in \mathcal{R}^{n_\nu \times (2n_c+n_d n_s)}$ contains the frictional wrenches (with the friction cone linearized into n_d directions for each surface contact). The rigid body non-penetration constraint and linearized Coulomb friction law then result in a set of complementarity conditions.

The uncertainty in support pressure distribution and continuous nature of the surface contact makes it difficult to model the system. However, if we model the support by three frictional point contacts, we can find the normal force distribution based on a out-of-plane force balance, and use the maximum allowable frictional forces resulting from these normal forces in our MLCP formulation. For the purposes of simulation and modeling, the manipulator can be considered an arbitrary convex polygon in the plane with position p_m. Because of our choice to use a three-point support approximating pressure distribution, the part can in fact be any planar polygonal shape.

System Parameters

There are several parameters present in the simulation model that affect the mechanics of the manipulation task and are unknown. These are:

μ_s Coefficient of surface friction.
μ_t Coefficient of manipulator-part friction.
$\underline{r_s}$ A 3×2 matrix specifying the support-point locations

The coefficients of friction μ_s and μ_t are constrained to the range $[0.0, 1.0]$. Support-point locations must obviously lie within the dimensions of the part being modeled. Additionally, their convex hull must include the part's center-of-mass so that the appropriate normal force at each support point can be calculated. The set of parameters is an 8-dimensional parameter space. The goal is to find the point in the parameter space and the neighborhood of the point that most closely characterize the uncertainty.

EXPERIMENTAL SETUP

Micro-manipulation Test-bed

The experimental setup consists of an inverted optical microscope (Nikon Eclipse TEU2000-U), 4-axis micro-manipulator (Siskiyou Design Instruments MX7600R), con-

troller (Siskiyou Design Instruments MC2000), 25 μm tip tungsten probe (needle), CCD camera (Sony XC-77), and control computer (Figure 2). There is a 4X objective on the microscope along with a 0.6X optical coupler producing a field of view (FOV) of 3.37 mm x 2.52 mm. The CCD camera records the images in the FOV and sends them to the control computer at 30 Hz. The micro-manipulator and controller allows incremental motion as small as 0.1 μm in 4 axes - X,Y,Z, and tool axes, respectively. Each axis has a range of motion of 20 mm and can be actuated with speeds ranging from 1.6 μm/sec to 1.7 mm/sec. During the experiments, the speed for each axis is fixed to 140 μm/sec.

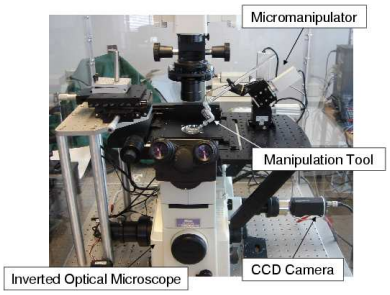

Figure 2. Experimental Setup

A fixture and part were made out of beryllium copper using a photochemical machining (PCM) process (sometimes referred to as chemical milling or chemical etching). This technique is useful for manufacturing high-precision flat metal parts. A photographically prepared mask, generated from a simple CAD drawing, is used to protect the metal that is to remain after the chemical etching process, while the unwanted materials are etched away [31]. The beryllium copper material, used for the fixture and part, is 1.5 mil (0.0015") thick.

The fixture has a rectangular section etched out of it that is 0.641" $\times$ 0.454" (1.63 mm $\times$ 1.15 mm). A polycarbonate film, 1 mil (0.01") thick, is fastened to the bottom of the fixture to allow for a transparent surface where the part sliding can reside. This transparent quality is needed here since the light source for the inverted microscope is projected up from underneath the fixture. For traditional systems with a camera mounted opposite to the light source, this transparent quality of the fixture backing is not needed. The rectangular cut-out coupled with the polycarbonate film backing provides an area where the characterization experiments are performed.

Various size parts were manufactured through the PCM process. The particular one used for the characterization tests is 0.064" x 0.033" (1621 μm $\times$ 842μm) in size. During the chemical etching process, a lead is attached to the part fixing it to the sheet of beryllium copper so that it doesn't wash away. When the part is later removed from the sheet, a tab remains where the lead was severed. This tab, 0.0068" $\times$ 0.0023" (173 μm $\times$ 53 μm), is small in size when compared to the other dimensions of the part. Figure 3 shows the part and probe in the FOV of the microscope. Note that the probe is modeled as a polygon with a 25 μm side. During the experiments contact between the probe and part occurs at one of the vertices on this side (point contact) or with the side (line contact).

Due to the small size and mass of the part, the inertial forces do not dominate during these planar pushing operations [27]. For our system, we have estimated the inertial forces to be on the order of nano-newtons for the accelerations involved, while the frictional forces are estimated to be on the order of micro-newtons. Therefore, it is reasonable to assume the frictional forces dominate and to adopt a quasi-static framework.

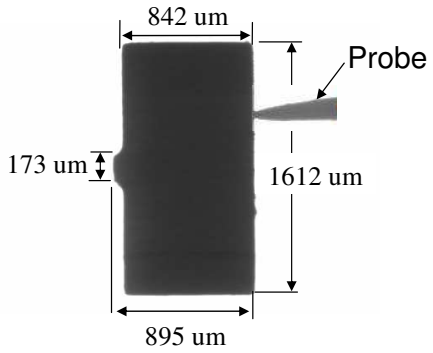

Figure 3. Peg in microscope FOV

Image processing techniques are applied to the images from the microscope to track the position of the part and probe during each experiment. Thresholding is used to initially produce an image where the part and probe pixels are black while everything else is white. The image is then processed further by using the geometry of the image to identify the pixels belonging to the probe and removing them from the filtered image. During this process, the coordinates of the tip of the probe are identified. An ellipsoid is fitted to the resulting blob image yielding the centroid and orientation of the part in each image frame.

Simulator

We have developed a software tool specifically designed to provide a simulation environment well suited for design and planning tasks that require accuracy and flexibility [32]. It employs a plug-in architecture so that modules can be substituted for a variety of motion models (first-order, quasi-static, dynamic) and time-stepping methods. Most importantly, it provides for rapid development of design optimization or motion planning algorithms while providing the ability to easily choose the appropriate dynamic modeling for a given application.

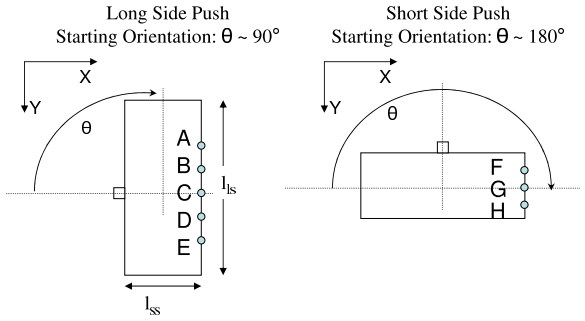

Figure 4. Nominal initial conditions of part for manipulation tests.

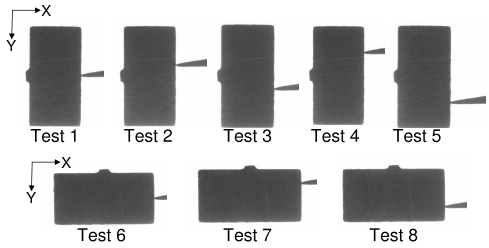

Figure 5. Starting configurations of probe for manipulation tests.

SYSTEM IDENTIFICATION

Design of Experiments

Eight sets of manipulation tests were used to identify and characterize the parameters in the 8-dimensional parameter space. Manipulation tests consisted of horizontal moves with contact between the probe and the part over distances of approximately 700 μm, executed on both the long and short side of the part. Figure 4 shows schematics of the part in its nominal initial conditions for each set of tests. The coordinate system is chosen to align it with that of the images obtained from the vision system. Pushes were made on the long side of the part at 5 nominal positions - at the midpoint of the side (Figure 4, pt.C), midpoint + $l_{ls}/4$ (pt.B), midpoint - $l_{ls}/4$ (pt.D), midpoint + $l_{ls}/2$ (pt.A), and midpoint - $l_{ls}/2$ (pt.E), where l_{ls} corresponds to the length of the long side of the part. For these pushes, the part was nominally placed at angle of 90°. The short side pushes were located at 3 nominal positions - at the midpoint (pt.G), midpoint + $l_{ss}/2$ (pt.F), and midpoint - $l_{ss}/2$ (pt.H), where l_{ss} corresponds to the length of the short side of the part. These pushes start with the part nominally placed at angle of 180°. Each of the starting configurations for the probe in each of the eight manipulation tests are shown in Figure 5. A minimum of three trials for each manipulation test were executed.

Estimation Algorithm

Given experimental data consisting of trajectories for each of the manipulation test experiments described above, what is the parameter vector $\mathbf{p}$, consisting of μ_s, μ_t, and $\underline{r_s}$, that best explains the experimental data? Our estimation algorithm estimates parameters such that the simulated manipulation test results match the experimental results from the execution of real manipulation tests as well as possible. Because the manipulated part's motion is a non-convex and non-smooth function of the system parameters, we cannot use gradient methods for optimization. This limits us to optimization algorithms that rely only on the evaluation of an objective function at different points.

The objective function we are interested in minimizing is related to the fitting of simulation to experiments over several trial test manipulation runs. For each trial, $\mathbf{x}_i$, and a given parameter vector, $\mathbf{p}$, we compute the simulated motion, $\mathbf{s}_i$, and compute the root-mean-squared error along each axes x, y, θ (with θ scaled by the characteristic length of the part to normalize). This creates a three dimensional error vector that we take the L_∞-norm of to get a quality measure for a single trial-simulation fit. When fitting across several experimental trials, the total objective becomes the average of quality measures across all trials.

$$f(\mathbf{x}_i,\mathbf{p}) = \left\| \sqrt{\frac{1}{T}\sum_{t=1}^{T}(\mathbf{x}_i(t)-\mathbf{s}_i(\mathbf{p},t))^2} \right\|_\infty \tag{3}$$

$$F(\mathbf{p}) = \frac{1}{N}\sum_{i=1}^{N} f(\mathbf{x}_i,\mathbf{p}) \tag{4}$$

It should be noted that a single evaluation of $F(\mathbf{p})$ requires N individual simulations.

The Nelder-Mead algorithm [33] (also known as the downhill simplex method) is a common method used for solving nonlinear optimization problems when the objective function is non-differentiable. The algorithm uses a $dim(p)+1$ simplex to find locally optimal solutions through successive evaluations of an objective function and transformations of points on the simplex. We initialize the algorithm with a value of $\mathbf{p}$ based on random valid support point locations and coefficients of friction. Our objective function $F(\mathbf{p})$ is customized to return arbitrarily large values when given a parameter choice $\mathbf{p}$ that violates the constraints. The algorithm is stopped when the simplex size (measured as the average distance from simplex center to each point) goes below a threshold. This is an adequate stopping criteria as the algorithm contracts the simplex when it finds a minimum.

Since the Nelder-Mead method is a downhill search technique, it can be stuck in local minima and fail to find the globally optimal solution. In order to reduce this possibility, we initialize the algorithm with several different random points in the parameter space. Since we believe the parameter space may have multiple points that closely match the experiments, this practice has the added benefit of finding several good parameter selections that can be used to help characterize the model uncertainties that a manipulation planning algorithm will have to consider.

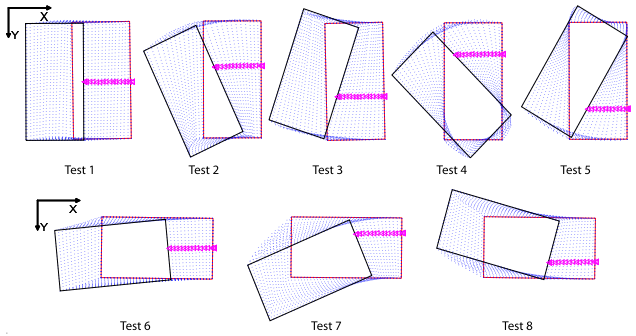

Figure 6. Snapshots from experimental data for trajectories obtained from selected manipulation tests.

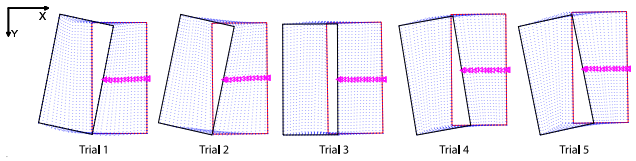

Figure 7. Trajectories for manipulation Test 1.

EXPERIMENTAL RESULTS

Experimental Errors

At least three trials for each manipulation test were performed. Figure 6 shows typical trajectories for one trial of each of the eight tests. The starting and ending configuration of the part are shown in solid lines, while the intermediate steps are pictured with dotted lines. The probe tip locations are represented with triangles. The trajectories for each of the trials were not all the same. They were consistent for the most part, but for certain starting configurations small variations from the nominal starting configuration of the part and probe can produce substantial changes in the resulting trajectory.

For each manipulation test performed, the X trajectory of the parts all showed the best correlation between the trials, while the Y and θ trajectories appear coupled and comprise most of the trajectory errors.

Test 1 is an example of a manipulation test that is sensitive to initial conditions, as shown in Figure 7. This test involves pushing at the midpoint of the long side of the rectangular part. A horizontal push directly at the center of mass of the part should intuitively result in a pure translation, as seen in the figure for Trial 3. In general, small perturbations from this starting configuration will yield either clockwise or counter-clockwise rotations for the same nominal test as seen in Trials 1, 2, 4, and 5. Most of this can be attributed to errors from the nominal starting position at the beginning of the tests. The accuracy of the vision system is conservatively estimated to be +/- 1 pixel, which corresponds to position measurement errors of the probe and the part of roughly +/- 5 μm and angular measurements of roughly +/- 0.005° error.

Figure 8(a) demonstrates the experimental trajectories of

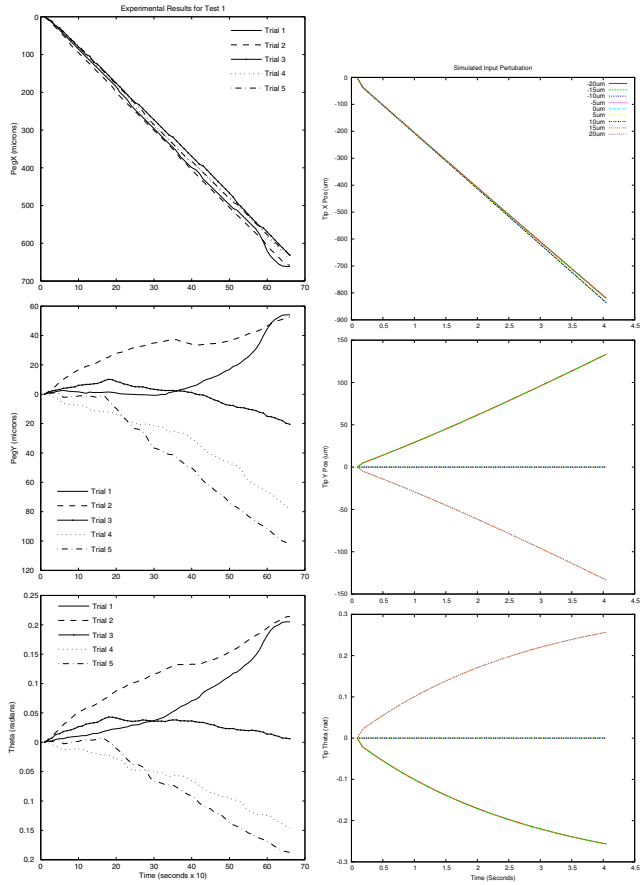

(a) Experimental (b) Simulation

Figure 8. Manipulation test showing large sensitivity to small errors in initial configuration.

Test 1, that should result in a pure translation but actually produce a wide range of rotations. However, as we can see from Figure 8(b), our model and therefore the simulation predict this sensitivity. When the simulator is presented with initial conditions for the part that lie in a neighborhood of within 5μm and 0.005° of the nominal position, the resulting trajectories exhibit a variation that is similar to that observed experimentally. Because the outcome is more sensitive to small errors in initial configuration, it is clear such pathological initial conditions should be avoided for manipulation planning.

Parameter Estimation

We used experimental results from manipulation tests that were generally repeatable - avoiding ”pathological” configurations. Our Nelder-Mead based estimation algorithm is able to match simulated trajectories to experimental trials with average root-mean-squared error of 20 to 40 μm in position and of 1 to

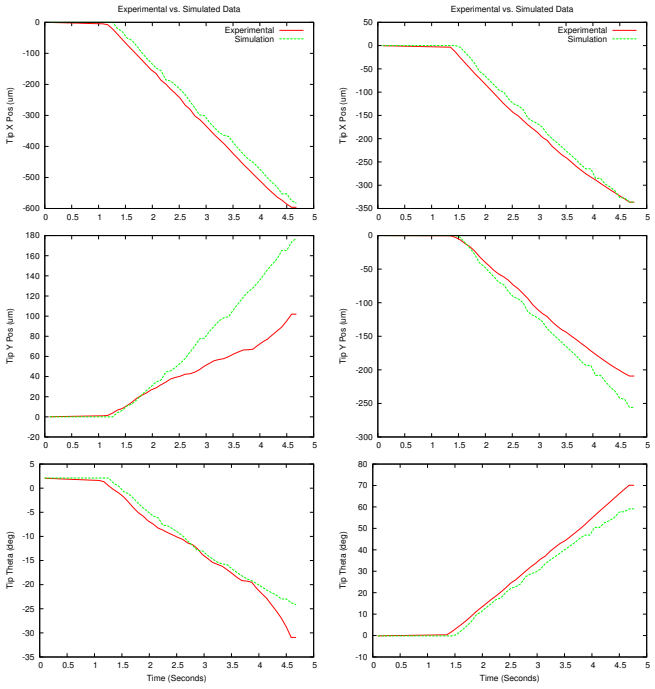

(a) Trial 1 (b) Trial 2

Figure 9. Simulator vs. Experimental Data with $\mathbf{p}_1^*$.

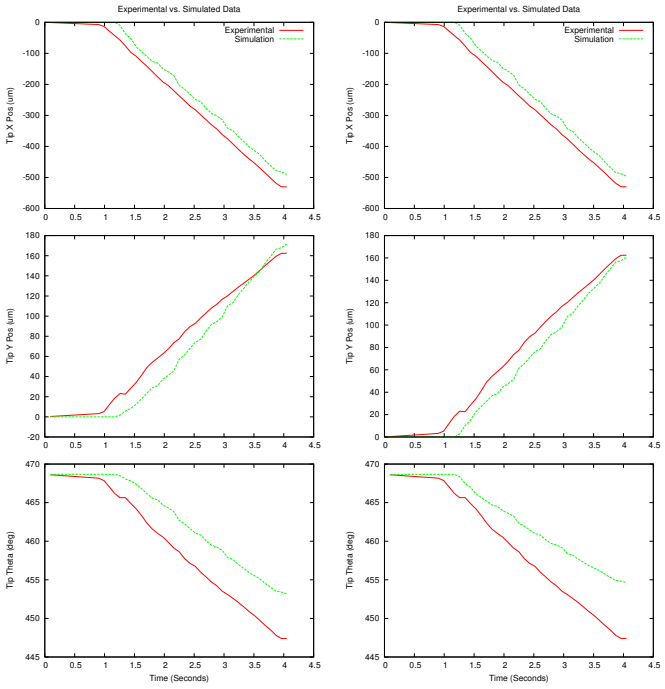

(a) $\mathbf{p}_1^*$ (b) $\mathbf{p}_2^*$

Figure 10. Simulator vs. experimental data with a manipulation not used for estimation.

3 degrees in orientation. The failure to obtain more accurate matches across large sets of trials could be partially attributed to measurement errors, not only the $5\mu m$, 0.005° error in measuring the trajectories, but also the effect of these errors in estimating the initial configuration. However, it is also likely that failures are the result of inconsistencies in the supporting surface.

By initializing the estimation algorithm with several random parameter choices, the algorithm often discovers more than one local minima in the parameter space. One choice of parameters can closely match some experimental trials while another choice can match other trials well.

For a concrete illustration of the result from parameter estimation, we performed a simple parameter estimation using two experimental tests as input (Tests 3 and 4 from Figure 6). We initialized the algorithm with two random sets of parameters $\mathbf{p}$ and found two possible solutions $\mathbf{p}_1^*$ and $\mathbf{p}_2^*$ (Table 1). Figure 9 shows the error between experiment and simulation for the trials involved in matching when using $\mathbf{p}_1^*$. As an additional test of the quality of $\mathbf{p}_1^*$ and $\mathbf{p}_2^*$, Figure 10 shows the result of simulating another trial (Test 8 in Figure 6) that was *not* used for parameter estimation.

The convergence for each execution of the estimation algorithm is shown in Figure 11. The uncertainty of the locally optimal parameter solutions is approximated by the size of the Nelder-Mead simplex which is also the stopping criteria of our

Table 1. Estimated Parameter Values for Example

	$\mathbf{p}_1^*$	$\mathbf{p}_2^*$
$\underline{r_s}$ (μm)	$(411.3, -563.3)$ $(-409.1, 605.9)$ $(-273.2, -102.1)$	$(-412.4, 794.0)$ $(-217.8, 774.5)$ $(278.8, -538.8)$
μ_t	0.666	0.536
μ_s	0.757	0.013

implementation and set to 10 μm in this case. Specific values for $\mathbf{p}_1^*$ and $\mathbf{p}_2^*$ are shown in Table 1 and Figure 12. Although the parameter sets $\mathbf{p}_1^*$ and $\mathbf{p}_2^*$ are distinct, they are qualitatively similar since they produce trajectories with comparable errors from experimental trajectories (Figure 10).

The solutions $\mathbf{p}_1^*$ and $\mathbf{p}_2^*$ are similar but have a large discrepancy in the value of μ_s. In fact, we observed that in simulation the value of μ_s has minimal affect on the trajectory of the part. This is due to the fact that it is the distribution of support force and not the coefficient of surface friction that will affect the motion. Since we cannot sense the force being applied by the probe, we cannot observe the actual frictional forces being exerted.

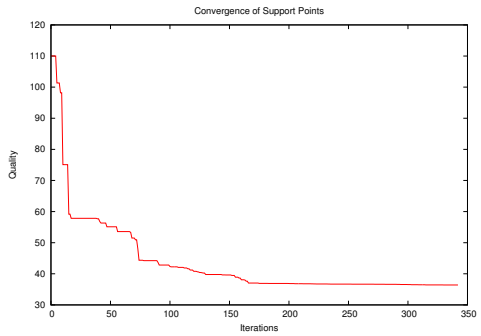

(a) Convergence for $\mathbf{p}_1^*$

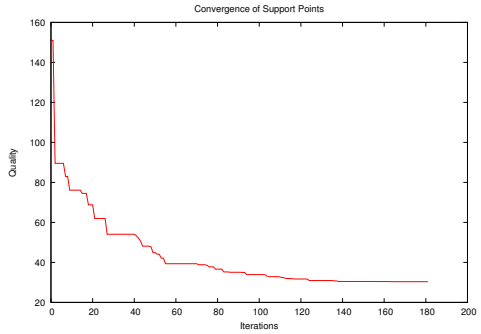

(b) Convergence for $\mathbf{p}_2^*$

Figure 11. Convergence of estimation algorithm.

DISCUSSION

A good understanding of grasping and manipulation for meso-scale assembly at the millimeter and sub-millimeter length scales requires a good characterization of the mechanics of manipulation and the uncertainty associated with frictional contact interactions. This paper describes an experimental approach to modeling the mechanics of frictional contact with applications to manipulating and assembling planar parts with a single probe. Though we used a specific probe and part geometry for this work, our characterization method and the quasi-static modeling approach is valid for other geometries.

The main finding of the paper is the fact that the trajectories generated by simulating the experimentally derived model of the force distribution and coefficients of friction match experimental trials with a root-mean-squared error of 20-40μm over a 600μm motion of the probe. Smaller motion of the probe result in smaller errors. We were also able to identify special cases in which manipulation tests have outcomes that are overly sensitive to initial starting conditions. These special cases are predicted by our simulator and observed experimentally.

Our results are the first step toward creating models for quasi-static, vision-guided meso-scale manipulation. Application of the model to generate motion plans for assembly is discussed in [4]. Indeed preliminary results show that this approach

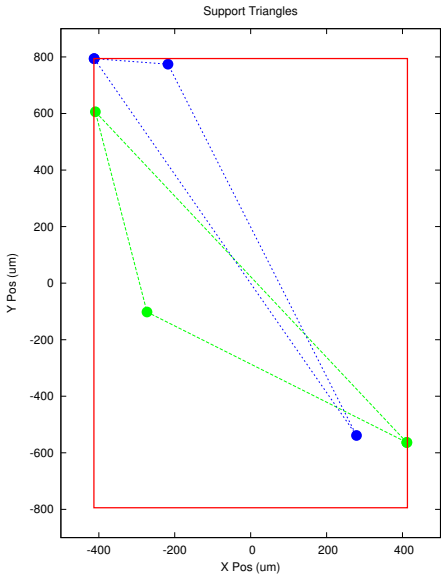

Figure 12. Support point locations for $\mathbf{p}_1^*$ and $\mathbf{p}_2^*$

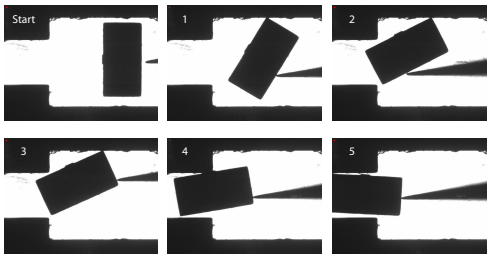

Figure 13. Manipulation task: Preliminary experimental results obtained from a plan generated by the model in Table 1

is promising for simple manipulation tasks. An example of the application of this approach is shown in Figure 13. The plan for assembling the part was generated automatically based on the model derived in this paper and the snapshots shown in the figure were taken during the execution of this plan. Because the clearance between the 1612 $\mu m \times$ 842 μm rectangular part and the slot is 137μm, it is possible to use our approximate model for successful assembly. Indeed our approach yields a 100% success rate in such tasks. However, it is clear that tighter tolerance tasks will require better models. Modeling and planning continue to remain an area of interest for future work.

ACKNOWLEDGMENT

This work was supported by NSF grants DMS01-39747, IIS-0413138 and IIS02-22927.

REFERENCES

[1] Goldberg, K., 1993. "Orientating polygonal parts without sensing". *Algorithmica*, **10**(2/3/4), August/September/October, pp. 210–225.

[2] Erdmann, M., and Mason, M., 1998. "An exploration of sensorless manipulation". *IEEE Journal of Robotics and Automation*, **4**(4), August.

[3] Moll, M., Goldberg, K., Erdmann, M., and Fearing, R., 2002. "Orienting micro-scale parts with squeeze and roll primitives". *IEEE Int. Conf. on Robotics and Automation, Washington, DC*, May 11-15.

[4] Cappelleri, D., Fink, J., Mukundakrishnan, B., Kumar, V., and Trinkle, J., 2006. "Designing open-loop plans for planar micro-manipulation". *IEEE Int. Conf. on Robotics and Automation, Orlando, FL*, May.

[5] Cecil, J., Vasquez, D., and Powell, D., 2005. "A review of gripping and manipulation techniques for micro-assembly applications". *International Journal of Production Research*, **43**(4), February, pp. 819–828.

[6] Feddema, J., Xavier, P., and Brown, R., 1999. "Micro-assembly planning with van der waals force". *Proceedings of the IEEE International Symposium on Assembly and Task Planning (ISATP '99)*, July, pp. 32 –38.

[7] Zhou, Y., and Nelson, B. J., 2000. "The effects of material properties and gripping force on micrograsping". *Proceedings of the 2000 IEEE International Conference on Robotics and Automation*, April, pp. 1115–19.

[8] Keller, C. G., 1998. "Micro grippers with intergrated actuator and force sensors". *Proceedings of the World Automation Congress, Anchorage, Alaska*, May 10-14, pp. ISORA–064.1 to 064.6.

[9] Cecil, J., and Gobinath, N., 2005. "Development of a virtual and physical cell to assemble micro devices". *Special Issue of the Journal of Robotics and CIM*, August-October, pp. 431–441.

[10] Alex, J., Vikramaditya, B., and Nelson, B. J., 1998. "A virtual reality teleoperator interface for assembly of hybrid mems prototypes". *Proceedings of DETC98 1998 ASME Engineering Technical Conference, Atlanta, GA*, Sept. 13-16.

[11] Kasaya, T., Miyazaki, H., Saito, S., and Sato, T., 1999. "Micro object handling under sem by vision-based automatic control". *Proceedings of the IEEE International conference on Robotics and Automation, Detroit, MI*, pp. 2189–2196.

[12] Mason, M., 1982. "Manipulator grasping and pushing operations". PhD thesis, Massachusetts Institute of Technology.

[13] Mason, M., 1986. "Mechanics and planning of manipulator pushing operations". *International Journal of Robotics Research*, **5**(3), pp. 53–71.

[14] Peshkin, M., and Sanderson, A., 1985. The motion of a pushed, sliding object, part1: Sliding friction. Tech. Rep. CMU-RI-TR-85-18, Robotics Institute, Carnegie Mellon University, Pittsburgh, PA, September.

[15] Song, P., Pang, J., and Kumar, V., 2004. "A semi-implicit time-stepping model for frictional compliant contact problems". *International Journal for Numerical Methods in Engineering*, Accepted for publication.

[16] Trinkle, J., Berard, S., and Pang, J., 2005. "A time-stepping scheme for quasistatic multibody systems". *International Symposium of Assembly and Task Planning*, July.

[17] Lynch, K., 1992. "The mechanics of fine manipulation by pushing". *IEEE Int. Conf. on Robotics and Automation, Nice, France*, May, pp. 2269–2276.

[18] Alexander, J., and Maddocks, J., 1993. "Bounds on the friction-dominated motion of a pushed object". *The International Journal of Robotics Research*, **12**(3), June, pp. 231–248.

[19] Pham, D., Cheung, K., and Yeo, S., 1990. "Initial motion of a rectangular object being pushed or pulled". *IEEE Int. Conf. on Robotics and Automation*, **1046-1050**.

[20] Lynch, K., and Mason, M., 1996. "Stable pushing: Mechanics, controllability, and planning". *International Journal of Robotics Research*, **15**(6), December, pp. 553–556.

[21] Salganicoff, M., Metta, G., Oddera, A., and Sandini, G., 1993b. "A vision-based learning method for pushing manipulation". *AAAI Fall Symp. on Machine Learning in Computer Vision.*

[22] Akella, S., and Mason, M. T., 1998. "Posing polygonal objects in the plane by pushing". *International Journal of Robotics Research*, **17**(1), Jan., pp. 70–88.

[23] Agarwal, P., Latombe, J., Motwani, R., and Raghavan, P., 1997. "Nonholonomic path planning for pushing a disk among obstacles". *IEEE Int. Conf. on Robotics and Automation*.

[24] Ben-Shahar, O., and Rivlin, E., 1998. "To push or not to push: On the arrangement of movable objects by a mobile robot". *IEEE Transactions on Systems, Man, and Cybernetics-Part B: Cybernetics*, **28**(5), October, pp. 667–679.

[25] Balorda, Z., 1990. "Reducing uncertainty of objects by robot pushing". *IEEE Int. Conf. on Robotics and Automation*, pp. 1051–1056.

[26] Fearing, R., 1995. "Survey of sticking effects for micro parts handling". *IEEE/RSJ Int. Conf. on Intelligent Robotics and Sys.(IROS), Pittsburgh, PA*, **2**, August 5-9, pp. 212–217.

[27] Boehringer, K., R.Fearing, and Goldberg, K., 1999. *Handbook of Industrial Robotics, 2nd Ed.* John Wiley and Sons, ch. Microassembly, pp. 1045–1066.

[28] Menciassi, A., Eisinberg, A., Izzo, I., and Dario, P., 2004. "From "macro" to "micro" manipulation: Models and experiments". *IEEE/ASME Transactions on Mechatronics*, **9**(2), June, pp. 311–320.

[29] Lynch, K., 1993. "Estimating the friction parameters of

pushed objects". *Proc. 1993 IEEE/RSJ Int. Conf.*, July.
[30] Yoshikawa, T., and Kurisu, M., 1991. "Identification of the center of friction from pushing an object by a mobile robot". *IEEE/RSJ International Workshop on Intelligent Robots and Systems IROS*, November.
[31] www.fotofab.com, 2006.
[32] Berard, S., Nguyen, B., Fink, J., Trinkle, J. C., and Kumar, V., 2006. Davinci code physical simulation library. To Be Released (http://www.cs.rpi.edu/ sberard/dvc).
[33] Nelder, J., and Mead, R., 1965. "A simplex method for function minimization". *Computer Journal,* **7**, pp. 308–315.